FATIGUE CRACK PROPAGATION UNDER VARIOUS TYPES OF LOADING

S. Machida*, M. Toyosada and T. Okamoto****

**Department of Naval Architecture, Faculty of Engineering, University of Tokyo, Bunkyo-ku, Tokyo, Japan*

***Technical Research Institute, Hitachi Zosen Corporation, Sakai-city, Osaka, Japan*

ABSTRACT

A model of fatigue crack propagation was developed with consideration of the behaviour of crack opening and closing during the part of cycles and the limiting stress at which no cumulative cyclic plastic energy has occured, namely "consuming stress". The effects of stress ratio and over- and/or under-spike load on fatigue crack propagation were analyzed by using the model. An example of ΔK_{th} value under zero-to-tension stress condition was also calculated by using the model. The results show the good agreement with expriments.

KEYWORDS

Fatigue crack propagation; crack opening and closing; "Consuming stress"; stress ratio; over- and/or under-spike loading; Dugdale model; threshold stress intensity factor.

INTRODUCTION

Fatigue cracks remain closed during part of the load cycle under fatigue loading. Newman (Newman, 1984) introduced the calculation model of the crack opening and closing phenomenon which was based on the Dugdale model (Dugdale, 1960), but was modified to leave plastically-deformed materials along the crack surfaces as the crack advances.

In his model, he neglected the stress-redistribution on the crack line in the calculation of Elber's crack opening load (Elber, 1971). Moreover he also neglected the elastic deformation for the materials along the crack surface. In this paper, Newman's calculation model is modified to take those neglected problems into consideration. Moreover we considered that a fatigue crack does not propagate if a local part in the vicinity of a crack tip remains elastic, i.e., a plastic strain does not accumulate at a crack tip. This limiting stress is named "consuming stress S_{CS}" which is replacing and corresponding with a crack opening stress S_{open} proposed by Elber.

Fatigue crack propagation tests using center notched tension test specimens were carried out under constant amplitude loading with various kinds of stress ratios and over- and/or under-spike loading conditions, for the purpose of confirming the effectiveness of our model.

CALCULATION MODEL OF CRACK OPENING AND CLOSING

The closure model is schematically shown in Fig. 1 which is similar to Newman's model[1]. For simplicity, a crack on an infinity wide plate subjected to uniform tension is analyzed.

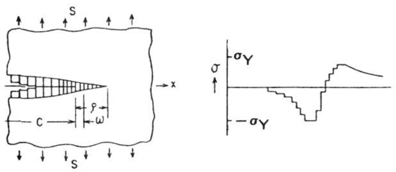

Fig. 1 Crack surface displacement and stress distributions along crack line

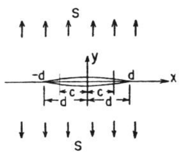

Fig. 2 Crackin an infinite width elastic plate subjected to uniform tension loading

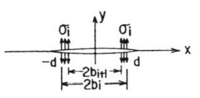

Fig. 3 Crack in an infinite width elastic plate subjected to partially loading

'he crack-opening displacement V(x) for the configuration shown in Fig. 2 is given by

$$V(x) = \frac{2(1-\eta^2)S}{E}\sqrt{d^2-x^2} = S\cdot f(x) \qquad (1)$$

or $|x|\leq d$, where $\eta=\nu$ for plane strain and $\eta=0$ for plane stress. The crack-opening displacement or the configuration shown in Fig. 3 is given by

$$V(x) = \frac{2(1-\eta^2)\sigma_i}{\pi E}\left[(b-x)\cosh^{-1}\left|\frac{d^2-bx}{d(b-x)}\right| + \sqrt{d^2-x^2}\,\sin^{-1}\frac{b}{d}\right]_{b=b_{i+1}}^{b=b_i} = \sigma_i\cdot g(b_i, x) \qquad (2)$$

or $|x|\leq d$. The equations which govern the response of the complete system are obtained by re-uiring that compatibility be met between the elastic plate and all of the bar elements which are erfect elastic-plastic bodies along the crack surface and plastic-zone boundary. The displacements or the configuration shown in Fig. 1 is

$$V(x) = S\cdot f(x) - \sum_{i=1}^{n} \sigma_i\cdot g(b_i, x) \qquad (3)$$

rom Eq.(3), the displacements at the center of the j-th bar element is

$$V(x_j) = S\cdot f(x_j) - \sum_{i=1}^{n} \sigma_i\cdot g(b_i, x_j) \qquad (j=1, \cdots, n) \qquad (4)$$

'here n is the total number of the bar elements and $x_j = (b_j + b_{j+1})/2$. The value of d is the fictitious alf crack length, that is, a half crack length plus tensile plastic zone, which is given as follows.

$$d_m = C_m/\cos\left(\frac{\pi S max_m}{2\,\sigma_Y}\right)$$

$$d = \max(d_m) \qquad (5)$$

here d_m : maximum fictitious half crack length at a certain time
$Smax_m$: maximum stress at a certain time
C_m : half crack length at a certain time
σ_Y : yield stress

he gage length L_j of the bar elements at x_j remains constant given by

$$L_j = V(x_j)\left(1 - \frac{\sigma_Y}{E}\right) \qquad (6)$$

hen only elastic stress acts on the bar. The gage length of the bar element will change as follows, hen the bar becomes plastic,

$$L_j = \begin{cases} V(x_j)\left(1 - \frac{\sigma_Y}{E}\right) \ldots \text{(acting tensile yield stress)} \\ V(x_j)\left(1 + \frac{\sigma_Y}{E}\right) \ldots \text{(acting compressive yield stress)} \end{cases} \qquad (7)$$

accordance with the recurrence calculation result of COD $V(x_j)$. The length of the j-th bar element with a elastic stress σ_j is

$$\ell_j = L_j\left(1 + \frac{\sigma_j}{E}\right) \qquad (8)$$

ι the region of contact zone within the fictitious crack, ℓ_j corresponds to $V(x_j)$. From Eq.(4) and q.(8), following equations are obtained,

$$L_j\left(1 + \frac{\sigma_j}{E}\right) = S\cdot f(x_j) - \sum_{i=1}^{n} \sigma_i\cdot g(b_i, x_i) \qquad (j=1, \cdots, n) \qquad (9)$$

where σ_i becomes zero in the crack opening region. From Eq.(9), the following iterative equations are obtained,

$$[\sigma_j]_{k+1} = \left\{S\cdot f(x_j) - \sum_{i=1}^{j-1}[\sigma_i]_{k+1}\cdot g(b_i,x_j) - \sum_{i=j+1}^{n}[\sigma_i]_k\cdot g(b_i,x_j) - L_j\right\} \Big/ \left\{g(b_j,x_j) + \frac{L_j}{E}\right\} \qquad (10)$$

where (k+1) is the current iteration number. Equations (10) are solved with the following constraints:

For elements in the plastic-zone ($x_j > C$),
if $\sigma_j > \sigma_Y$, set $\sigma_j = \sigma_Y$, (11)
if $\sigma_j < -\sigma_Y$, set $\sigma_j = -\sigma_Y$ (12)

For elements along the crack surface ($x_j \leq C$),
if $\sigma_j > 0$, set $\sigma_j = 0$, (13)
if $\sigma_j < -\sigma_Y$, set $\sigma_j = -\sigma_Y$

These constraints are due to elements separation and compressive yielding. In solving Eq.(10), $V(x_j)$ in the plastic zone at the maximum stress has to be first obtained by using Dugdale model and then L_j is set by Eq.(6). After that, crack growth is simulated by extending the crack by small incremental value. Making initial guess for $[\sigma_j]_1$, iterative calculations are made using equation (10). At every iteration, the stresses $[\sigma_j]_k$ are checked against the constraint conditions (11) through (13), and are updated, if necessary. This is repeated until $[\sigma_j]_{k+1}$ become $[\sigma_j]_k$. COD V(x) are obtained by Eq.(3).

A fatigue crack may not propagate, if a local part of a crack tip, i.e., the bar element at the crack tip remains elestic, because a plastic strain does not accumulate. Let this limiting stress be called "con-suming stress S_{CS}" in this paper. The numeral identifying the bar element at the crack tip is m and the length of the bar element at S_{CS} is

$$\ell = L_m\left(1 + \frac{\sigma_Y}{E}\right) \qquad (14)$$

Then from Eq.(9), the following iterative equations are obtained.

$$\left.\begin{aligned} &\text{For } j \neq m,\\ &[\sigma_j]_{k+1} = \Big\{[S_{CS}]_k\cdot f(x_j) - \sigma_m\cdot g(b_m, x_j) - \sum_{\substack{i=1\\ i\neq m}}^{j-1}[\sigma_i]_{k+1}\cdot g(b_i, x_j) \\ &\qquad - \sum_{\substack{i=j+1\\ i\neq m}}^{n}[\sigma_i]_k\cdot g(b_i, x_j) - L_j\Big\} \Big/ \left\{g(b_j, x_j) + L_j/E\right\} \\ &\text{For } j = m,\\ &[S_{CS}]_{k+1} = \Big\{L_m\left(1 + \frac{\sigma_Y}{E}\right) + \sigma_m\cdot g(b_m, x_m) + \sum_{\substack{i=1\\ i\neq m}}^{n}[\sigma_i]_{k+1}\cdot g(b_i, x_m)\Big\} \Big/ f(x_m) \end{aligned}\right\} \qquad (15)$$

S_{CS} value is calculated in the similar way of solving Eq.(10).

In the present computation, the plastic zone and the wake zone were arbitrarily divided into 25 graduated bar elements except the bar at the tip. The smallest element was located at the crack tip and had the width ($=b_m - b_{m-1}$) of 0.005mm which was sufficiently small to calculate S_{CS} accurately.

Now let us consider the phenomenon of fatigue crack propagation for under- and over-spike loading. Fig. 4 shows schematically crack opening and closing phenomenon during fatigue crack propagation under constant amplitude loading including an under-spike loading. A local part ahead and in the vicinity of a crack tip is stretched in the transverse direction to a crack line due to tensile yielding at a maximum stress. When small amount of a crack grows at a maximum stress, elastic stress is partially released at the location of the newly generated crack surfaces and then, the new crack opens a little due to the released elastic stress at the maximum stress. Therefore the new crack may close at a little lower stress than the maximum stress under unloading process. Then the crack may close over the certain area in the vicinity of the crack tip at a minimum stress as shown in condition (3) in Fig. 4. Condition (2) corresponds to the state with the stress of S_{CS} at which tensile plastic zone starts to be generated at the crack tip under loading process and then the effective stress range is given by the stress at condition (1) minus the stress at condition (2).

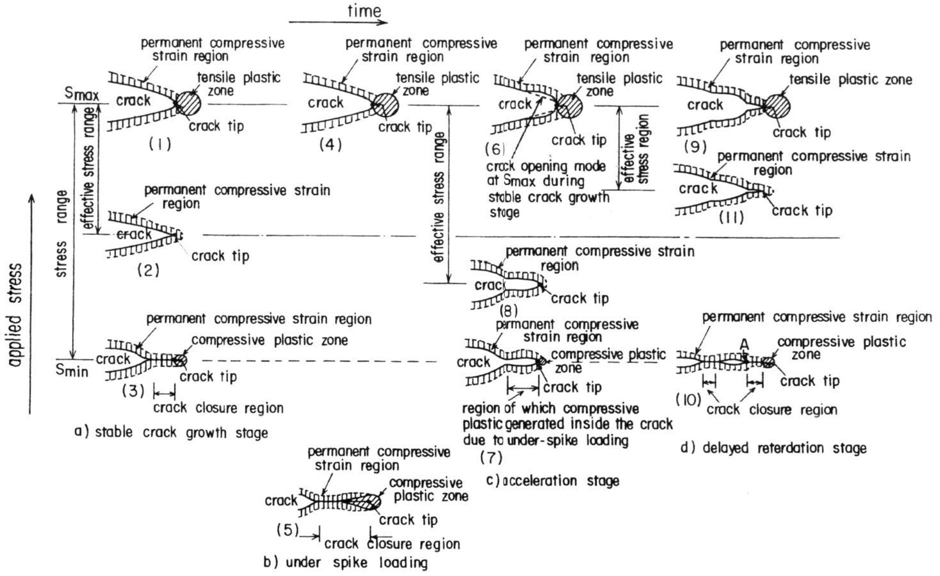

Fig. 4 Crack opening and closing during fatigue crack propagation due to under-spike loading

Jnder-spike loading leads to growing and streching a compressive yielding zone in the contact zone at minimum stress for under-spike loading (see condition (5) in Fig. 4). The crack opens in the ıanner of having dents in the vicinity of the crack tip at the maximum stress due to the compressive ielding zone for the under-spike loading (see condition (6)). Due to the dents, the crack may still pen at the minimum stress (see condition (7)). Under loading stress, then, a tensile plastic zone :arts to be generated at a little higher than the minimum stress and S_{CS} level may be lower than that nder stable crack propagation stage (see condition (8), cf. condition (2)). The effective stress range, $_{max}-S_{CS}$, in this stage becomes larger than that in the stable crack propagation stage. The crack is ıen expected to be accelerated.

/hen the crack propagates further, the shape of the crack opening at the maximum stress may be ke a cross sectional shape of the top part of "Gothic tower", as shown in condition (9). Unloading :ads to crack closure, as shown in condition (10) and the crack might occasionally touch at a region part from the crack tip in addition to the vicinity of the crack tip. Just after reloading, stress may oncentrate at A point in Fig. 4-condition (10), which is inside the crack. Therefore S_{CS} may be ırger than that at the stable crack propagation stage, as shown in stage (d) (see condition (11)). 'hen $S_{max}-S_{CS}$, the effective stress range, at stage (d) is less than that at stage (a), and the delayed ;terdation of a fatigue crack propagation may occur.

.s the crack propagates further, the region affected by the under-spike loading moves away from ıe crack tip, and the effective stress range increases and approaches to that at stage (a).

igure 5 shows a schematic view of crack opening and closing phenomenon during fatigue crack ropagation under constant amplitude loading including over-spike loading. Similar phenomenon to nder-spike loading occurs in this case. But the affective zone due to over-spike loading is greater ıan that due to under-spike loading. As a result, the effect of over-spike loading on fatigue crack ropagation may be larger than that of under-spike loading.

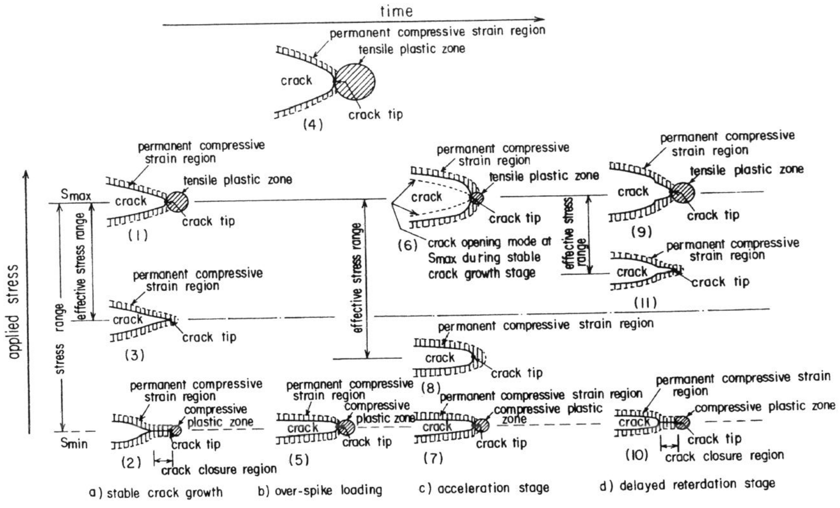

Fig. 5 Crack opening and closing during fatigue crack propagation due to over-spike loading

RESULTS AND ANALYSIS OF FATIGUE CRACK PROPAGATION TEST

Figure 6 shows the specimen configurations and the material used is mild steel of which chemical compositions and mechanical properties are shown in Table 1. Table 2 shows the testing conditions including the conditions of constant amplitude loading with various stress ratio and with various spike loading.

The test results of constant amplitude loading with various stress ratios are shown in Fig. 7. It shows that fatigue crack propagation rates increase as stress ratios increase. Figure 8 shows the calculated S_{CS} for various stress ratios using above model. The results show that S_{CS} value increases as a crack advances until it reaches a cretain length, and then increase in S_{CS}

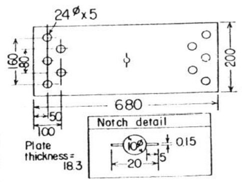

Fig. 6 Test specimen

Table 1 Chemical composition and mechanical properties

Chemical composition (%)					Mechanical properties			
C	Si	Mn	P	S	Yield stress (kgf/mm²)	Tensile stress (kgf/mm²)	Elongation (%)	Reduction of area (%)
0.14	0.05	0.98	0.014	0.003	31.0	48.3	31.5	70.8

Table 2 Test condition

Specimen No	Test	Stress ratio R	Stress (kgf/mm²)
CCT-1	Const. amplitude	0.1	0.68 ~ 6.8
CCT-2	Spike load	0.3	3.0 ~ 10.1
CCT-3	Spike load	0.5	5.46 ~ 10.93
CCT-4	Spike load	0.3	3.0 ~ 10.11
CCT-5	Const. amplitude	0.65	11.4 ~ 17.5
CCT-6	Const. amplitude	0.3	3.26 ~ 10.9
CCT-7	Const. amplitude	0.1	0.75 ~ 7.47
CCT-9	Const. amplitude	0.5	4.76 ~ 9.51

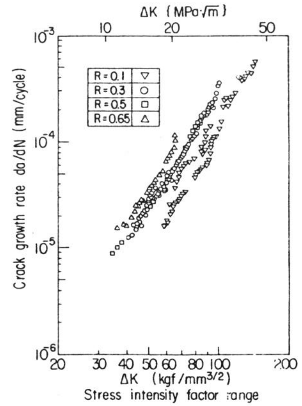

Fig. 7 Crack propagation characteristics on various stress ratios

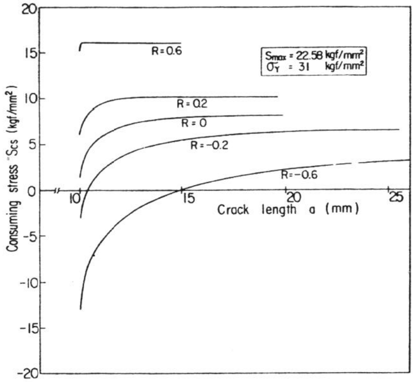

Fig. 8 Consuming stress variation at each stress ratio

becomes very gradual and finally S_{CS} maintains almost constant as the crack advances. The sharp increase in S_{CS} in early stage of crack propagation may lead to no existance of compressive plastic deformation at the first time in the wake zone. Figure 9 shows the relation between stress intensity factor range ΔK divided by yield stress and U value which is the ratio of the effective stress range ΔS_{eff} to the applied stress range, for various kind of materials with different yield stresses and Young's moduli. Figure 10 shows the re-arranged results of the fatigue crack propagation rate in the basis of the effective stress intensity factor

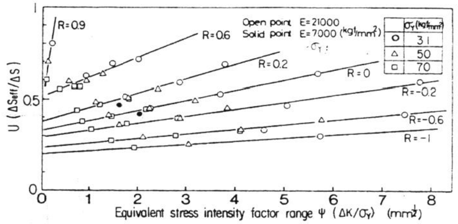

Fig. 9 Effective stress range for the equivalent stress intensity factor range

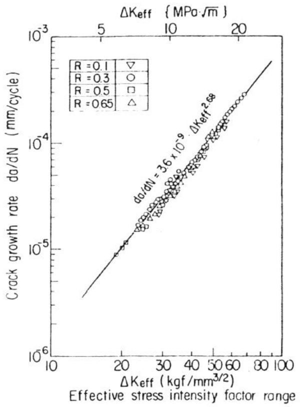

Fig. 10 Crack growth rate by effective stress intensity range at each stress ratio

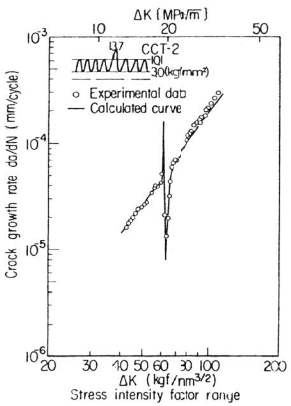

Fig. 11 Crack growth rate characteristics on an overloading

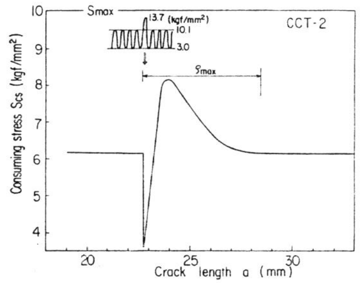

Fig. 12 Consuming stress change with crack growth on an overloading

range ΔK_{eff} $(=(S_{max}-S_{cs})\sqrt{\pi a}\ f(a)$, f(a): correction factor) by using Fig. 9. This results show that fatigue crack propagation rates are mainly given as a function of ΔK_{eff} and Fig. 9 is available to predict the effect of fatigue crack propagation rates on stress ratios.

Figure 11 shows the experimental fatigue crack growth rate of specimen CCT-2 in which a single over-spike loading is applied. Figure 12 is the calculated result of S_{cs} for specimen CCT-2. From the calculated result of S_{cs}, ΔK_{eff} is obtained and the prediction of the fatigue crack propagation rate is given as shown by the solid line in Fig. 11 from Fig. 9 and Fig. 10. The predicted fatigue growth rate is in good agreement with the experimental fatigue growth rate except in the region of accelerated fatigue crack propagation. In this region, growth rate could not be measured because of the measurement interval of crack length of 1 mm in the test. Experimental results as compared with the predicted propagation life curve are shown in Fig. 13. The predicted propagation life is fairly in good agreement with experimental one.

Figure 14 shows the fatigue crack growth rate data and the predicted propagation rate for specimen CCT-3 in which a single under-spike loading is applied as shown in Table 2. It also shows that the predected growth rate on the bases of S_{cs} concept is in good agreement with the experimental one. It is clear by comparison between Fig. 11 and Fig. 14 that delayed reterdation zone due to an under-spike loading is smaller than that due to an over-spike loading.

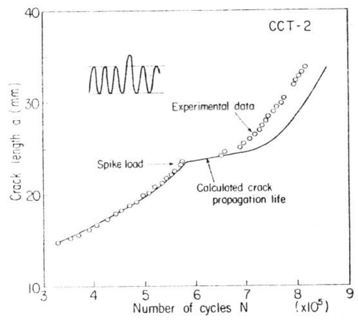

Fig. 13 Crack propagation life on an overloading

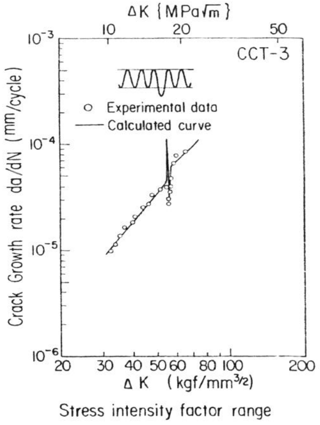

Fig. 14 Crack growth rate characteristics on an underloading

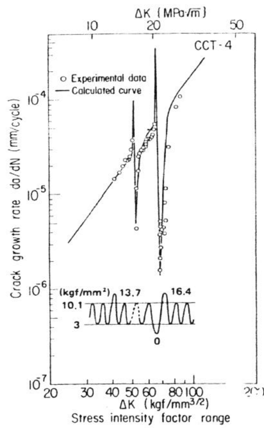

Fig. 15 Crack growth rate characteristics on an overloading after an underloading

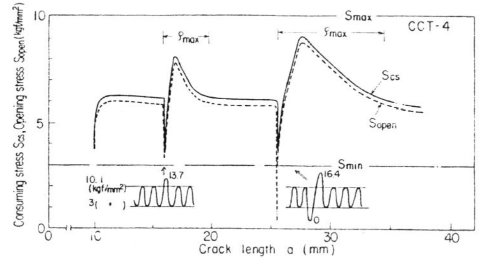

Fig. 16 Consuming stress and opening stress changes with crack growth on an overloading or an overloading after an underloading

Figure 15 shows the fatigue crack growth rate for specimen CCT-4 in which a single over-spike loading is applied and then an overload is applied just after an underload is applied.

The calculated result of S_{CS} value for specimen CCT-4 in shown in Fig. 16. Calculated result of crack opening stress S_{open}, which corresponds to an applied stress at which stress acting the bar element at a crack tip in the model come to zero during re-loading process, is also shown in the figure. The general trend of the change of S_{open} with crack growth due to spike-loadings seems to be similar to that of S_{CS}. Moreover the value of S_{open} is almost the same as the S_{CS}, but is little less than S_{CS}. The prediction of the crack growth rate for specimen CCT-4 using the S_{CS} value in Fig. 16 is shown by a solid line in Fig. 15 which is in good agreement with the experimental value.

Figure 17 shows the crack propagation life for specimen CCT-4. The experimental life agrees better with the predected life due to S_{CS} than that due to S_{open}.

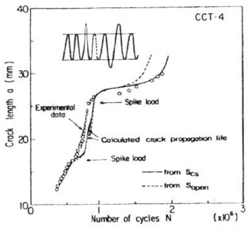

Fig. 17 Crack propagation life on an overloading or an overloading after an underloading

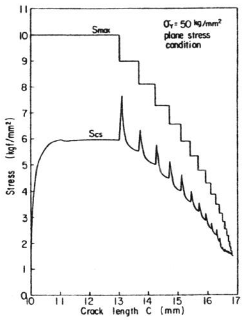

Fig. 18 Changes of S_{CS} value as a crack advances under step down loading

Figure 18 shows an example of the calculated S_{CS} value in the case of a decreasing step loading with the stress ratio of zero, simulating a ΔK_{th} test. As shown in Fig. 18, S_{CS} value finally becomes equal to S_{max} and then fatigue crack is supposed not to propagate any more. From the result, the ΔK_{th} value was obtained to be 22 kgf $\cdot$ mm$^{-\frac{3}{2}}$ $\{6.8\text{MPa}\sqrt{\text{m}}\}$. It seems that the calculated ΔK_{th} values are in good agreement with previous experimental ones.

From above results, our model is available to predect fatigue crack propagation life under various types of loading.

CONCLUSION

An analytical fatigue crack-closure model is developed and used in a crack-growth analysis program by proposing the concept which a fatigue crack does not propagate if a local part in the vicinity of a crack tip remains elastic and the limit stress is named "consuming stress S_{CS}" in place of S_{open} concept by Elber to predict crack growth under various kinds of loading. The model was introduced to modify the analytical crack growth model by Newman. The proposed model needs only one fatigue crack growth data under constant amplitude loading for a material to predict fatigue growth life under other general loading. On the contrary, Newman's model needs at least data from four loadings.

The present model correlated the constant amplitude data over a wide range of stress ratio quite well. The model also predicted well the effects of load intereraction, such as retardation and acceleration. Moreover, ΔK_{th} value can be expected to be calculated by the model.

REFERENCES

Dugdale, D.S. (1960). Yielding of Steel Sheets Containing Slits. J. Mech. Phys. Solids, 8.

Elber, W (1971). The Significance of Fatigue Crack Closure. ASTM STP486, 230.

Newman, J.C. (1981). A Crack-Closure Model for Predicting Fatigue Crack Growth under Aircraft Spectrum Loading. NASA Tech. Memo. 81941.